

Step Initiation and Propagation Rate Minima in Solution Crystallization of Five Long Alkanes

Edy G. R. Putra and Goran Ungar*

Department of Engineering Materials, University of Sheffield, Sheffield S1 3JD, U.K.

Received March 20, 2003

Revised Manuscript Received April 18, 2003

Introduction. Studies of long *n*-alkanes continue to provide new information on the crystallization mechanism of polymers.¹ The stochastic attachment to the growth face of competing molecular conformations is exposed strikingly by the occurrence of crystallization rate minima at transitions between E and F2^{2,3} or F2 and F3⁴ growth modes. Here E, F2, and F3 denote extended, folded-in-two, and folded-in-three chain conformations. The “self-poisoning” mechanism, initially proposed to explain the minimum,² has received support from rate equation treatment based on a simple “fine-grain” model as well as from Monte Carlo simulation.⁵ The initial experimental studies have provided only an empirical “crystallization rate” parameter, i.e., a complex mix of nucleation and growth rates.^{2–4} Since then pure growth rate has been measured in melt crystallization experiments, using optical microscopy,^{6,7} confirming that the minimum indeed occurs in both the rates of growth and primary nucleation.⁶

In the case of solution crystallization, direct growth rate measurement has so far been reported only on one alkane, C₁₉₈H₃₉₈.⁸ The minimum in growth rate as a function of crystallization temperature T_c was confirmed. In addition, a minimum was also observed as a function of concentration *c*, with crystal growth rate increasing with decreasing solution concentration and exhibiting a negative reaction order as low as -5 . For phenyldecane solutions at $T_c = 98.0$ °C the minimum is located at $c = 3.0$ wt %. The rate equation model again gave a good semiquantitative agreement with the experiment.⁸

In the course of our studies of long alkanes, we have observed, and reported on the examples of C₁₆₂H₃₂₆⁹ and C₂₄₆H₄₉₄,¹⁰ that crystal habit changes drastically as the growth minimum is approached. Therefore, for a meaningful quantitative description of the growth kinetics, it is not sufficient to determine just any “growth rate”, but instead growth rates of individual crystallographic faces must be determined separately. In long alkanes, as in polyethylene, these rates are G_{110} and G_{100} , referring to {110} and {100} faces (see Figure 1). Second, since the curvature of some faces¹⁹ has been successfully described mathematically in terms of the step initiation rate (*i*) and step propagation rate (*g*),^{11–13} these kinetic parameters can now also be determined. We have undertaken a comprehensive in situ study of solution crystallization kinetics and morphology on a range of alkanes. In this preliminary report we summarize the data on temperature dependence of G_{110} , G_{100} , i_{100} , and g_{100} for a range of alkanes from C₁₆₂H₃₂₆

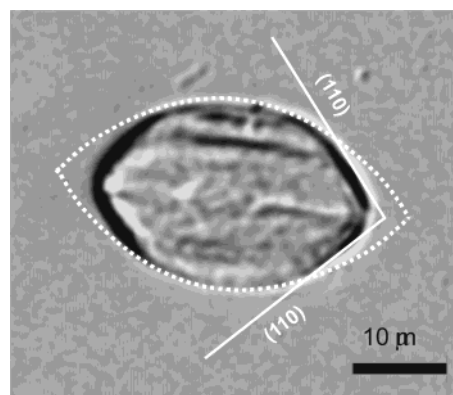


Figure 1. An example of fitting a corrected Mansfield ellipse (white dotted line) to {100} faces of a C₂₄₆H₄₉₄ crystal ($T_c = 116.3$ °C, 4.75% initial concentration). $ib_0^2/2g = 0.31$. The solid white lines are extrapolations of the {110} faces.

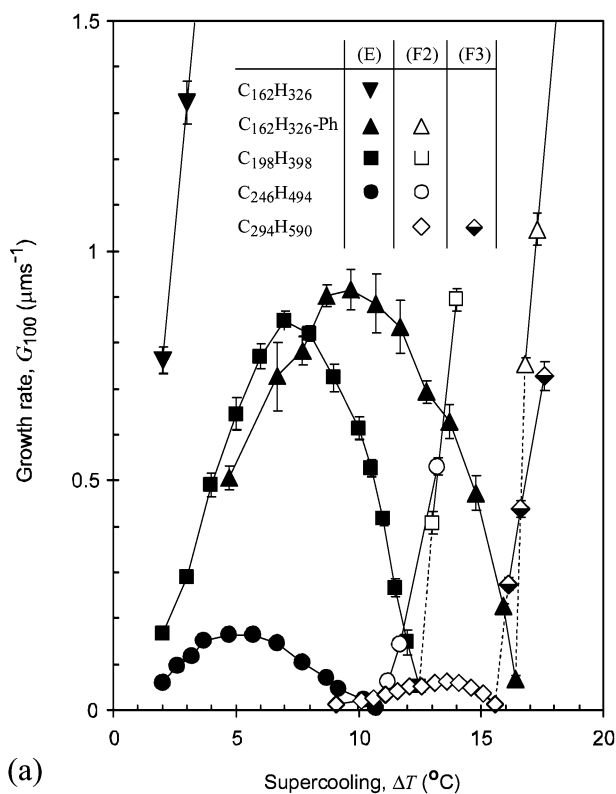
to C₂₉₄H₅₉₀. The full analysis will be published elsewhere, starting with C₂₄₆H₄₉₄.¹⁰

Experimental Section. Pure *n*-alkanes C₁₆₂H₃₂₆, C₁₉₈H₃₉₈, C₂₄₆H₄₉₄, and C₂₉₄H₅₉₀, used in this study, were synthesized by Dr. G. M. Brooke and co-workers at the University of Durham.¹⁴ Solutions in the range of 5% were made in *n*-octacosane (Sigma-Aldrich), and aliquots were placed between 0.1 mm thick, 6 mm diameter coverslips. In the case of C₁₆₂H₃₂₆ 0.97% solutions in 1-phenyldecane were also studied, since crystallization rates from octacosane were too fast for reliable measurements at higher supercoolings. A specially designed two-stage T-jump cell was used in combination with an interference-contrast Olympus BX 50 optical microscope, a Coolsnap digital camera, and Image-Pro imaging software.¹⁰ A sequence of micrographs were recorded isothermally following a rapid sample transfer from the hot stage to the viewing stage set at T_c . It was ascertained through internal calibration that the temperature inside the solution dropped to within 0.1 °C of T_c in less than 2 s.¹⁰ Crystal growth rates were extrapolated to the first appearance of the crystals, i.e., to the initial concentration.⁸ Dissolution temperatures of folded and extended-chain crystals at a particular concentration were determined in situ at near zero heating rate. More experimental details are given in refs 9 and 10.

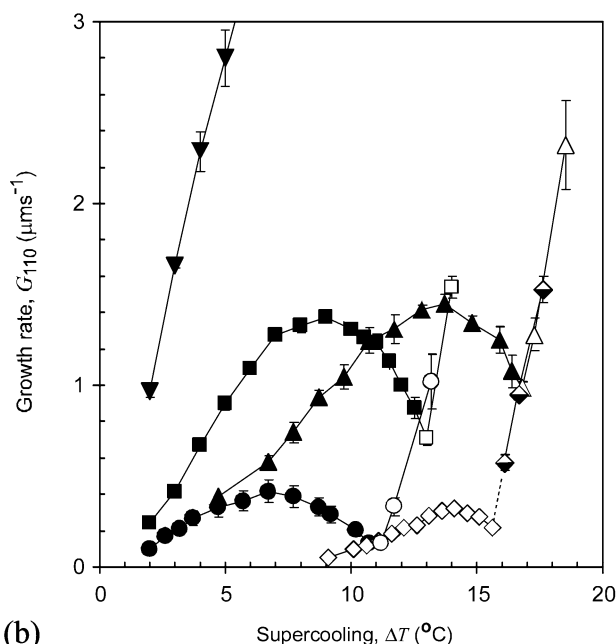
Results and Discussion. Figure 1 shows a typical truncated lozenge crystal (C₂₄₆H₄₉₄) with two curved {100} faces and four relatively straight {110} faces. Fitted to the {100} faces is a Mansfield ellipse,¹¹ modified for the pseudo-centered rectangular 2d lattice representative of alkanes.¹³ The truncated lozenge morphology persisted in all experiments described in this note, albeit with substantial variation in curvature of the {100} faces and in the length ratio of the {110} and {100} faces. Only in the case of the 0.97% phenyldecane solution of C₁₆₂H₃₂₆ at low supercooling did we obtain nontruncated crystals. These were of the “*a*-axis lenticular” type, delimited exclusively by curved {110} faces.⁹

In Figure 2a G_{100} is plotted against supercooling ΔT for the five alkanes included in this study. ΔT is defined with reference to the final dissolution temperature of extended-chain crystals at the relevant concentration. The dissolution temperatures of the extended and folded

* Corresponding author: e-mail G.Ungar@shef.ac.uk.



(a)



(b)

Figure 2. Initial crystal growth rates of the five alkanes indicated. (a) G_{100} , (b) G_{110} . Symbols: full, extended chains (E); empty, once-folded chains (F2); half-full, twice-folded chains (F3). Initial octacosane solution concentrations were as follows: $C_{162}H_{326}$, 4.62%; $C_{198}H_{398}$, 5.0%; $C_{246}H_{494}$, 4.75%; $C_{294}H_{590}$, 5.04%. Phenyldecane solution of $C_{162}H_{326}$: 0.97%. Each data point is an average of measurements on several crystals from a number of samples.

chain forms for the alkanes reported on here and for concentrations used are listed in Table 1. The difference between the dissolution temperatures of E and F2 forms is generally slightly larger than the difference between the corresponding melting points.¹⁵ This is attributed to the inability to anneal completely the metastable folded crystals without causing chain unfolding.

Table 1. Final Dissolution Temperatures of Extended and Folded Forms of *n*-Alkanes in 1-Phenyldecane and *n*-Octacosane

<i>n</i> -alkanes	<i>c</i> (w/w %)	T_d^E (°C)	T_d^{F2} (°C)	T_d^{F3} (°C)
in phenyldecane	0.97	102.1	85.7	
$C_{162}H_{326}$				
in octacosane				
$C_{162}H_{326}$	4.74	112.9	102.7	104.3
$C_{198}H_{398}$	5.0	114.9	108.3	
$C_{246}H_{494}$	4.75	118.5	112.2	
$C_{294}H_{590}$	5.04	120.8		

All alkanes exhibit a very deep minimum in G_{100} , bringing the growth virtually to a halt at the growth transition between E and F2 forms ($C_{162}H_{326}$, $C_{198}H_{398}$, $C_{246}H_{494}$) and between F2 and F3 forms ($C_{294}H_{590}$).

The G_{110} rates measured on the same crystals are shown in Figure 2b. Again all alkanes exhibit a rate minimum at the growth transitions. This time, however, the minimum is not as deep as in the case of G_{100} . In fact, the value of G_{110} at the growth rate minimum is typically between $2/3$ and $1/3$ that at the maximum. G_{110} is thus very much higher than G_{100} at and near the minimum, resulting in crystals grown in this temperature range being needlelike, highly elongated along *b*-axis, with the aspect ratio reaching 15:1.¹⁰

In all cases G_{100} is much more suppressed by self-poisoning at the minimum compared with G_{110} . It is thus the very strong inhibition in G_{100} that causes the particularly deep minimum noted in the overall solution crystallization rate of long alkanes.³ Such a disproportionate effect on G_{100} does not exist in melt crystallization,^{1,16} and hence the minimum in the overall rate of melt crystallization is less pronounced.

The decreasing G_{100}/G_{110} ratio (increasing truncation) with decreasing T_c is in stark contrast with the decreasing G_{100}/G_{110} ratio with increasing T_c observed in polyethylene.¹⁷ These opposing trends suggest that self-poisoning also takes place in crystallization of polyethylene, and increasingly so at increasing temperatures, as will be discussed elsewhere.¹⁰

A further point to note in Figure 2 is that, compared to the case of G_{110} , the $dG/d(\Delta T)$ gradient for G_{100} turns negative further above T_{min} ; thus, $T_{max} - T_{min}$ is approximately 4 °C for G_{110} and 6 °C for G_{100} for all alkanes in the E growth regime. In the F2 growth regime ($C_{294}H_{590}$) $T_{max} - T_{min}$ is less.

The analysis of the curvature of {100} faces in combination with G_{100} data yields the temperature dependence of i_{100} and g_{100} , shown for the five alkanes in Figure 3a,b. i_{100} is the rate of secondary nucleation, or step initiation, expressed as the number of successful nuclei per 1 μm length of the growth face per second. g_{100} is the rate of step propagation, or substrate completion, in $\mu m/s$. As can be seen in Figure 3, both i and g pass through a maximum and reach a minimum at the growth transition. The minimum in i is very much deeper than the minimum in g . While i falls to about 10^{-3} of its value at the maximum, the decline in g is relatively small ($1/3 < g_{min}/g_{max} < 3/4$). The consequence of the disparity between $i(T)$ and $g(T)$ is a drastic change from highly curved to faceted {100} lamellar edges as T_c decreases toward T_{min} . Combined with G_{110} remaining relatively high at T_{min} (Figure 2b), the resulting crystals grown at the minimum are narrow-ribbon-like, outlined by straight {100} facets.

The most highly suppressed process, and the overall rate-limiting one at the minimum, is thus the formation

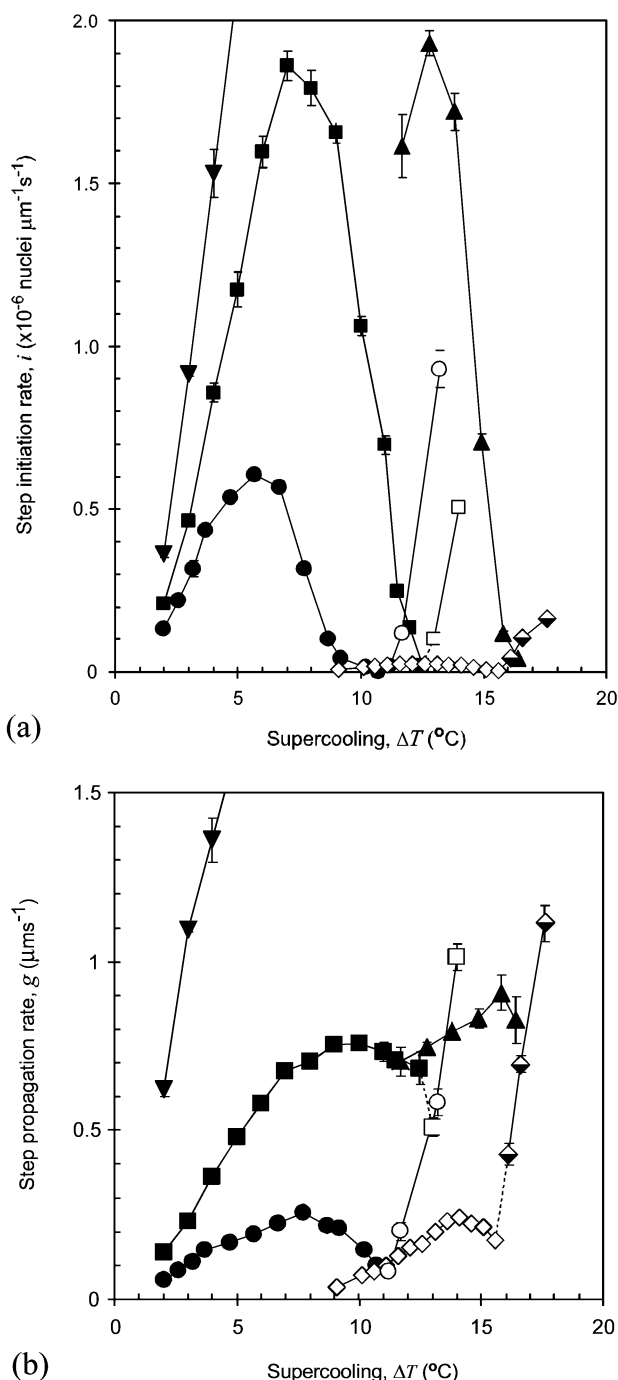


Figure 3. (a) Step initiation rate i and (b) propagation rate g on {100} faces of the five alkanes. Symbols are the same as in Figure 2. Crystals of $\text{C}_{162}\text{H}_{326}$ from phenyldecane did not show {100} faces at low supercooling.

of secondary nuclei on the {100} faces. The reason for {100} faces being more poisoned than {110} ones is not known at present. On the other hand, the reason that

layer initiation is more suppressed than layer propagation can be understood qualitatively in terms of competing low-barrier F2 depositions blocking E nucleation (or F3 depositions blocking F2 nucleation). As discussed in ref 10, the mere fact that a minimum in g exists at all contradicts the classical surface energy-based description of step propagation in polymer crystallization. According to that description, the barrier to step propagation ("substrate completion") is independent of the stem length and contains only the fold surface energy. Accordingly, F2 depositions would have a higher, not a lower, barrier than E depositions, and F2 depositions would not compete with E layer propagation. The fact that the latter process (g_{100}) is suppressed means that the layer propagation barrier is to a large extent entropic in nature, since this is always lower for shorter stems.¹⁸

Another intriguing finding of this work is the very highly suppressed step initiation in once-folded growth of $\text{C}_{294}\text{H}_{590}$ (Figure 3a). This and other points will be addressed elsewhere.

Acknowledgment. We are very grateful to Dr. G. M. Brooke for the alkane samples which were synthesized with financial support from EPSRC. This work was funded by the Petroleum Research Fund, administered through American Chemical Society, and by EPSRC.

References and Notes

- Ungar, G.; Zeng, X. B. *Chem. Rev.* **2001**, *101*, 4157.
- Ungar, G.; Keller, A. *Polymer* **1987**, *28*, 1899.
- Organ, S. J.; Ungar, G.; Keller, A. *Macromolecules* **1989**, *22*, 1995.
- Hobbs, J. K.; Hill, M. J.; Barham, P. J. *Polymer* **2001**, *42*, 2167.
- Higgs, P. G.; Ungar, G. *J. Chem. Phys.* **2001**, *114*, 6958.
- Organ, S. J.; Keller, A.; Hikosaka, M.; Ungar, G. *Polymer* **1996**, *37*, 2517.
- Sutton, S. J.; Vaughan, A. S.; Bassett, D. C. *Polymer* **1996**, *37*, 5735.
- Ungar, G.; Mandal, P.; Higgs, P. G.; de Silva, D. S. M.; Boda, E.; Chen, C. M. *Phys. Rev. Lett.* **2000**, *85*, 4397.
- Ungar, G.; Putra, E. G. R. *Macromolecules* **2001**, *34*, 5180.
- Putra, E. G. R.; Ungar, G. *Macromolecules*, submitted for publication.
- Mansfield, M. L. *Polymer* **1988**, *29*, 1755.
- Point, J. J.; Villers, D. *J. Cryst. Growth* **1991**, *114*, 228.
- Toda, A. *Faraday Discuss.* **1993**, *95*, 129.
- Brooke, G. M.; Burnett, S.; Mohammed, S.; Proctor, D.; Whiting, M. C. *J. Chem. Soc., Perkin Trans. 1* **1996**, 1635.
- Ungar, G.; Stejny, J.; Keller, A.; Bidd, I.; Whiting, M. C. *Science* **1985**, *229*, 386.
- de Silva, D. S. M. Thesis, University of Sheffield, 2002.
- Organ, S. J.; Keller, A. *J. Mater. Sci.* **1985**, *20*, 1571.
- Sadler, D. M. *Nature (London)* **1987**, *326*, 174.
- This applies to faces, such as {100} in polyethylene, which are bisected by a mirror plane normal to the lamella. For faces that lack this symmetry, e.g. {110} in polyethylene, no adequate quantitative model exists at present.⁹

MA034356H